

Model-Based Interpretation of Creep Profiles for the Assessment of Polymer-Mucin Interaction

Silvia Rossi,¹ M. Cristina Bonferoni,¹
Carla Caramella,^{1,3} Liliana Ironi,² and
Stefania Tentoni²

Received May 7, 1999; accepted June 7, 1999

Purpose. This paper presents a new rheological approach, based on a stationary viscoelastic test (creep test), to describe the interaction between a mucoadhesive polymer and mucin.

Methods. An automated model builder tool is used to identify accurate compliance models from experimental data. This approach is applied to study the interaction of gastric porcine mucin with three viscosity grades of a mucoadhesive polymer, sodium carboxymethylcellulose.

Results. By comparing the compliance models of polymer solutions and their mixtures with mucin, prepared at different concentrations and concentration ratios, we observed an increase in the order of the model of the mixtures at the lowest polymer concentration for all the three viscosity grades; this effect is more pronounced for the low viscosity grade. On the other hand, an increase in mucin concentration does not result in a further increase in model order, but rather in a decrease in retarded compliance and an increase in newtonian viscosity.

Conclusions. We interpret the model order as the number of different interactions between polymer and mucin, and the parameter values as a measure of their strength. The results indicate the suitability of the approach for a deep characterization of the interactions involved in mucoadhesion.

KEY WORDS: mucoadhesion; polymer-mucin interaction; creep test; automated mathematical modeling; compliance models; sodium carboxymethylcellulose.

INTRODUCTION

Since the 1980's a great effort has been devoted to the development of mucoadhesive drug delivery systems to improve drug therapy and bioavailability (1–9). Various theories have been proposed to explain the mechanism involved in the mucoadhesion phenomenon, the most common of which are the wetting-spreading theory and the interpenetration theory (10). It is recognized that both the ability of the adhesive to spread over the mucosa and the interpenetration of the polymer chains and mucus glycoproteins have to be considered to explain the phenomenon (5,11). In fact, the two processes should be involved in different stages of the interaction between mucoadhesive material and mucus. One process prevails over the other mainly due to the type of formulation (liquid, semisolid, solid). In particular, in presence of an already hydrated gel phase, the mucoadhesive joint is certainly strengthened by the interpenetration between hydrated polymer and mucin chains.

According to interpenetration theory, some authors considered the changes in the rheological properties that the mucoadhesive polymers undergo when mixed with mucus as a measure of the polymer-mucus interaction. Hassan and Gallo observed a synergistic increase in viscosity when a mucoadhesive polymer and mucin (the main component of mucus) were mixed together (12). They interpreted such an increase as an index of the extent of the mucoadhesive interaction. Further investigations on rheological properties of polymer-mucus (or mucin) mixtures were performed by several authors using dynamic viscoelastic analysis (13–16). They observed an increase in the viscoelastic properties of mucoadhesive gels when mixed with mucus or mucin. For different polymers a correlation was also found between rheological interaction parameters and the mucoadhesive strength obtained using tensile stress techniques (17–19).

These results confirm the suitability of the rheological approach to characterize the mucoadhesive interface. Moreover, it seems useful to provide more information about the structural changes that occur in the polymeric network as a result of the interaction with mucin.

This paper presents a new approach based on a stationary viscoelastic (creep) test. It is well known from linear viscoelastic theory that the creep compliance curves can be described by mathematical models which allow us to identify in the viscoelastic response of the material different components, each of them describes a specific physical feature. In the case of polymer-mucin mixtures, the model-based approach enables us to assess the material complexity and to relate it with the presence of different types of interactions (chain interlocking, chemical bonds) within the polymeric network, and consequently to get a deeper insight into the mechanism of mucoadhesion.

The main problem lies in the actual difficulties encountered in building models which “adequately and accurately” describe the observed creep compliance curve.

Rheology provides a framework (20) for building, under suitable assumptions, models of materials which exhibit complex behaviors when they are subjected to external forces. Within this framework, it is possible, in theory, to build a model at any level of complexity but, in practice, this is not feasible due to the difficulty in handling the symbolic procedures which must be applied to derive the final equation. Let us observe that the resulting models are equations between stress, strain and their time derivatives, i.e. Ordinary Differential Equations (ODE's), which, being “exact” relations between mathematical entities, describe the behaviors of ideal materials. Such equations constitute a reference model space where to search for the model of the behavior of an actual substance; the search process is driven by the experimental data.

Different kinds of knowledge are necessary to tackle the modeling problem as a whole: this has been a serious deterrent from using rheological models for the assessment of materials as it would have deserved.

Recent work has dealt with the development of a comprehensive environment for the automated formulation of an accurate model of an actual viscoelastic material in accordance with its observed response to standard experiments (21).

In this work we exploited the modelling tool to investigate the mucoadhesive interaction between a bioadhesive polymer,

¹ Department of Pharmaceutical Chemistry, University of Pavia, Pavia, Italy.

² Institute of Numerical Analysis - C.N.R., Pavia, Italy.

³ To whom correspondence should be addressed. (e-mail: caramella@chifar.unipv.it)

sodium carboxymethylcellulose (NaCMC), and a commercial porcine gastric mucin. More precisely, creep tests were performed on isoviscous aqueous solutions of three different viscosity grades of NaCMC and their mixtures with mucin. The experimental data have been processed through the automated modeling system, and their compliance models have been identified. The number of the model parameters and their values give a measure of the complexity of the material which may be related to both the different types of interactions occurring within the polymeric network and their strength. The model-based approach has also allowed us to evaluate the influence both of the viscosity grade and of polymer and mucin concentration on such interactions.

The polymer solutions and the mixtures were also subjected to dynamic oscillatory and viscosity tests, which are widely accepted methods for the assessment of polymer mucoadhesive properties; the results obtained agree with those derived by means of our model-based approach.

A BRIEF OVERVIEW ON CREEP TEST

Many materials show both elastic deformation and viscous irreversible deformation when they are subjected to an instantaneous constant shear stress, provided that sufficient time is allowed for the test and the stress is large enough to prevent the sample from showing only elasticity, but still within the limits of linear strain-stress relation.

A “stationary creep” experiment consists in applying a given constant shear stress s_0 over a time interval, and in observing the time course of the elicited strain response $e(t)$.

The creep “compliance” $J(t)$ is defined as $e(t)/s_0$. Figure 1 shows a typical creep compliance-time curve (A-B-C-D). It can be segmented into three regions according to the dominant behavior: instantaneous elasticity, retarded elasticity, and viscosity.

The total creep compliance $J(t)$ can be modeled as the sum of up to three basic contributions, each one corresponding to a behavior component:

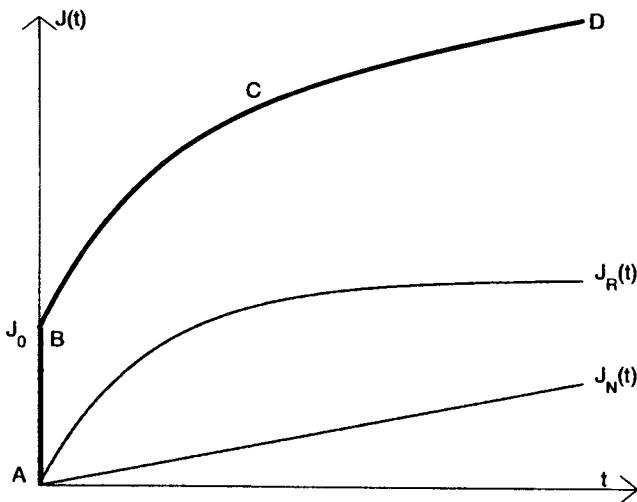


Fig. 1. Creep test: a typical compliance response (A-B-C-D) of a linear viscoelastic material, modeled as the sum of three components which account for instantaneous elasticity (J_0), retarded elasticity ($J_R(t)$) and viscosity ($J_N(t)$)

$$J(t) = J_0(t) + J_R(t) + J_N(t)$$

where:

1) $J_0(t)$ accounts for instantaneous elasticity (jump A-B in Fig. 1). If we assume that Hooke’s law of linear elasticity holds, then

$$J_0(t) = \text{constant} = \frac{1}{E_0}$$

where E_0 is the instantaneous elastic modulus. The instantaneous compliance J_0 can be ascribed to the prompt elastic stretching of bonds between the primary structural units of the system.

2) $J_R(t)$ accounts for viscous flow (linear region C-D in Fig. 1). If we assume that Newton’s law of linear viscosity holds, then

$$J_N(t) = \frac{1}{\eta_N} t$$

where η_N is the newtonian viscosity.

The newtonian compliance J_N can be ascribed to the rupture of bonds, either irreversible or such that the time for them to reform is much longer than the experiment duration.

3) $J_R(t)$ accounts for retarded elasticity (non-linear growth B-C in Fig. 1). One or more Voigt models, derived by combining in parallel the Hooke and the Newton models, are used to describe this behavior:

$$J_R(t) = \sum_{i=1}^n J_i \left(1 - \exp \left(-\frac{t}{\tau_i} \right) \right)$$

where τ_i are called “retardation times”, and n represents the model complexity (order). After the initial instant t_0 and before the viscous behavior becomes dominant, bonds break and reform, and consequently the produced deformation is slower but still recoverable. Bonds do not break and reform all at the same rate: the weaker ones break at smaller times than the stronger ones. Each term summing up to J_R is characterized by an asymptotic compliance value J_i and a retardation time τ_i .

MATERIALS AND METHODS

Materials

Three different viscosity grades of sodium carboxymethylcellulose (NaCMC) (Blanose®, Aqualon GmbH & Co K.G., Germany) were used:

- low viscosity grade (l.v.) 7LFD (66 kDa);
- medium viscosity grade (m.v.) 7M8FD (190 kDa);
- high viscosity grade (h.v.) 7HFD (440kDa).

Commercial porcine gastric mucin (type II, Sigma Chimica, Italy) was used as biological substrate. The use of both commercial and freshly prepared mucin samples involves advantages and drawbacks (22). A criticism raised against mucin employment is the sample variability. The results obtained in (22), where we had observed that NaCMC interaction properties did not change when the polymer, hydrated in distilled water, was mixed with two different commercial brands of porcine gastric mucin, justifies the use of a commercial mucin.

Sample Preparation

The polymers were hydrated at room temperature in distilled water. For all the polymers three concentration levels (low, medium and high) were prepared. The concentrations were chosen to obtain, at each level, isoviscous solutions (Table I).

Polymer solutions, after an overnight rest in refrigerator, were mixed with porcine gastric mucin to obtain mixtures containing polymers at the concentrations in Table I and 8% (w/w) mucin concentration. For the medium concentrations of the three polymers, mixtures at 6% and 10% (w/w) mucin concentrations were prepared. Polymer solutions were tested for rheological properties soon after their preparation and after an overnight rest in refrigerator. No variations in such properties were observed during the storage time.

Mucin dispersions in distilled water at 6%, 8% and 10% (w/w) were also prepared; their viscosities, calculated at 50 s⁻¹, were respectively 34 mPa.s, 72 mPa.s and 140 mPa.s.

Experimental Methods

Rheological Analysis

We performed rheological measurements by means of a CS Rheometer (Bohlin Instruments Division, UK). A coaxial cylinder combination (C25) and two cone-plate combinations (Cp4/20 and Cp4/40) were used as measuring systems. All measurements were carried out at 25°C after a rest time of three minutes.

Stationary Viscoelastic Measurements

Each sample was subjected to a rapid rise in shear stress from zero to a value chosen in the linear viscoelastic range, which was then held constant for a period of time sufficient to reach an irreversible deformation. The creep compliance $J(t)$ (Pa⁻¹) was recorded as a function of time. Each sample (single preparation) was tested at least five times to consider measure variability.

Dynamic Viscoelastic Measurements

Increasing values of shear stresses were applied to each sample at a constant frequency value (1 Hz). Storage modulus (G') and loss modulus (G'') were recorded as a function of the shear stress. The linear viscoelastic region, characterized by constant values of G' and G'' on increasing shear stress values, was identified for each sample examined. Each sample (single preparation) was tested three times.

Table I. Concentrations of Isoviscous Solutions of NaCMC of Different Molecular Weight

	low conc. (w/w) ^a	medium conc. (w/w) ^b	high conc. (w/w) ^c
lv grade	6.0%	7.0%	8.0%
mv grade	3.0%	3.4%	4.1%
hv grade	1.4%	1.6%	1.8%

^a The apparent viscosity, measured at 50s⁻¹, was about 0.9 Pa.s.

^b The apparent viscosity, measured at 50s⁻¹, was about 1.3 Pa.s.

^c The apparent viscosity, measured at 50s⁻¹, was about 3 Pa.s.

The following dynamic interaction parameters were calculated (15):

$$\Delta G' = G'_{\text{mix}} - G'_{\text{pol}}$$

$$\Delta G'' = G''_{\text{mix}} - G''_{\text{pol}}$$

where G'_{pol} and G''_{pol} are the storage and loss modulus (Pa) of the polymer solution, whereas G'_{mix} and G''_{mix} are the storage and loss modulus (Pa) of the mixture.

The dynamic interaction parameters were then normalized with respect to the values G' and G'' of the polymer solutions ($\Delta G'/G'_{\text{pol}}$, $\Delta G''/G''_{\text{pol}}$) to make it possible the comparison between the three grades.

Viscosity Measurements

The apparent viscosity was measured on each sample after application of 50 s⁻¹ shear rate for 1 min. The interaction parameter rheological synergism ($\Delta\eta$) was calculated as follows (12):

$$\Delta\eta = \eta_{\text{mix}} - (\eta_{\text{muc}} + \eta_{\text{pol}})$$

where η_{mix} is the apparent viscosity (Pa·s) of the mixture, η_{muc} is the apparent viscosity (Pa·s) of the mucin dispersion, η_{pol} is the apparent viscosity (Pa·s) of the polymer solution.

To allow for the comparison of the values of $\Delta\eta$ related to the different mixtures, they were normalized with respect to the viscosity of the polymer solution ($\Delta\eta/\eta_{\text{pol}}$).

Computational Methods

The computational environment, developed at IAN-CNR Pavia, automatically provides, as output, an accurate model of a real material, given as input experimental data. Its construction has required a variety of qualitative, numerical, statistical and model-based techniques (21). The overall modeling process, sketched in Fig. 2, proceeds in three main phases:

1. generation of an exhaustive library of models of ideal viscoelastic materials, which differ from each other in structural complexity;

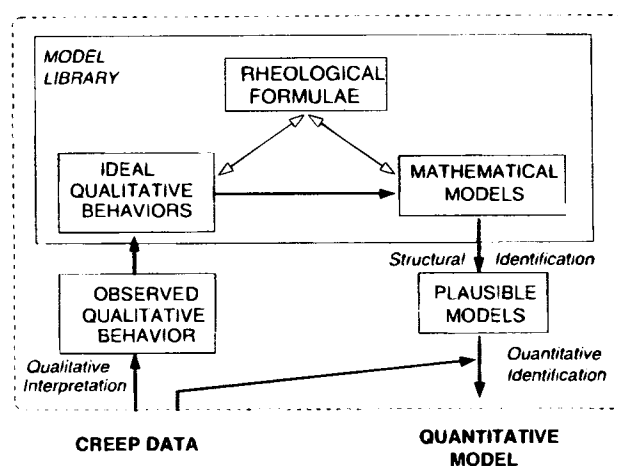


Fig. 2. Overview of the automated modeling system architecture: given experimental data as input, an accurate quantitative model of a material is provided as output.

2. identification, within the library, of a class of models the structure of which suitably captures the qualitative behavior of the material;

3. identification, within the selected class, of the equation, namely its order and the numeric values of its parameters, which refines the quantitative properties of the material.

The library generation (phase 1) is done once for all, and exploits a compositional approach provided by Rheology: models of materials are built by analogy to mechanical models. An analogical model is a series/parallel assembly of basic mechanical components reproducing the fundamental mechanical properties (elasticity and viscosity) whose overall behavior can be arbitrarily complex. In the rheological formalism, such analogical devices are represented by Rheological Formulas (RF's), whereas in the mathematical language they are represented by Ordinary Differential Equations (ODE's). The ODE's are built by exploiting suitable connection rules and mathematical models of the basic components (Hooke's and Newton's laws), and their structures characterize distinct viscoelastic behaviors.

The library of models is automatically generated following an enumerative procedure: all non-equivalent RF's, made up of n basic components ($n = 1, \dots, 20$ in the current implementation) variously connected in series or in parallel, are generated along with their corresponding ODE's. Each model, which represents a distinct ideal viscoelastic material, is then associated with its qualitative profile, i.e., a characterization of the simulated creep response in terms of physical features such as instantaneous and retarded elasticity, and viscosity. Such profiles play a key role for the structural identification of the real material (phase 2) since they serve as a standard of comparison with the qualitative profiles of the observed data which are abstracted through the geometric characterization of the basic physical features in the experimental curve. The match of the observed profile with those in the library gives as a result a class of equations, the "plausible models", that capture all and none but the physical features of the real material (Fig. 3).

Then, both the plausible model class and the experimental data are input to a quantitative identification loop (phase 3) aimed at identifying the simplest model which attains the maximum accuracy: plausible models of increasing complexity are evaluated on the basis of both their degree of fit to data and their complexity, within the limits of both numerical and statistical reliability (23).

More precisely, let us denote by k and θ the tentative model order and parameters, respectively; the discrepancy between the response $y(t_i; \theta)$ computed according to the model $M_k(\theta)$ and the mean experimental data z_i is measured by means of a weighted least squares estimator

$$d(\theta) = \sum_i \left(\frac{y(t_i; \theta)}{\sigma_i} \right)^2$$

where σ_i are suitable weights, which are derived from each set of data replicates and take into account measure variability. The optimal model fit is attained by minimizing $d(\theta)$ within a numerical well-conditioning region, which ensures that the system is identifiable (21,24). Model evaluation is then performed by exploiting the Akaike Information Criterion, which considers both the model fit and the model complexity. The loop ends when the optimal balance is attained. The result of such a process is a quantitative ODE model for the given

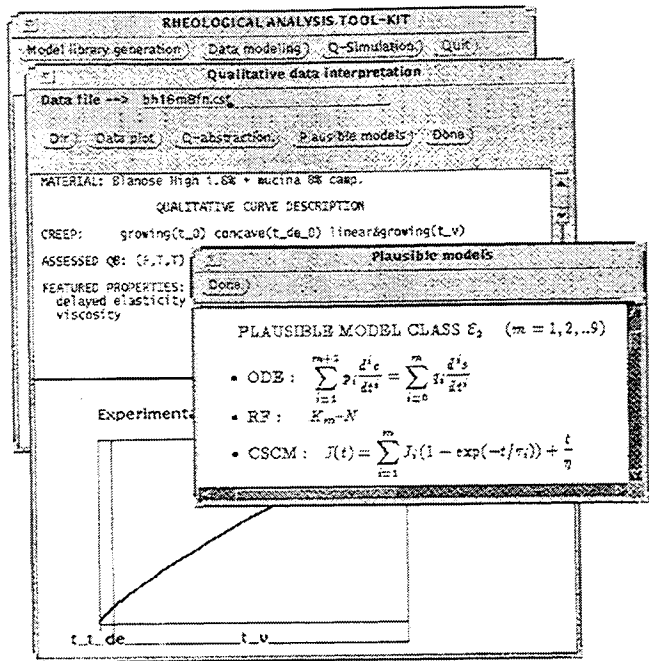


Fig. 3. Computer outcome of the qualitative analysis and plausible model class selection steps within the automated modeling process.

material, where both the order and the parameter values are known and characterize the tested material.

In the case of the stationary creep test ($s(t) = s_0$ constant), the tool provides plausible models also in the form of compliance models (CSCM in Fig. 3). Such models go through the identification step as well. The ultimate result of the modeling process is therefore: 1) an analogical model (RF), 2) a quantitative ODE model, and 3) a quantitative compliance model. This latter form is currently preferred because its parameters have a direct physical meaning.

RESULTS AND DISCUSSION

Stationary Viscoelastic Tests

The qualitative interpretation task, automatically performed on each creep data set, has highlighted the presence of delayed elasticity and viscosity only in all of the tested samples (see Fig. 3).

The class of candidate compliance models drawn out from the identification process is:

$$J(t) = \sum_{i=1}^n J_i \left(1 - \exp\left(-\frac{t}{\tau_i}\right) \right) + \frac{t}{\eta_N}$$

For each creep data set, values of n (model order), J_i , τ_i and η_N have been estimated. Tables II, III, and IV summarize the estimated values of n , J_i , and η_N , for the NaCMC solutions at different grades, and their mixtures with mucin at different concentrations. The τ_i values are not reported since they do not appear to add further information to that already captured by the other parameters.

Low Viscosity Grade (Table II)

The creep profiles of NaCMC l.v. grade solutions prepared at 6% and 7% (w/w) concentrations are well explained by

Table II. NaCMC Low Viscosity (l.v.) Grade: Model Order (n), Newtonian Viscosity (η_N), and Retarded Elastic Compliance Values (J_i , $i = 1, 2, 3$)

Sample	Model order n	Retarded elastic compliance (Pa^{-1})			Newtonian viscosity ($\text{Pa}\cdot\text{s}$) η_N
		J_1	J_2	J_3	
NaCMC 6% (w/w)	0	—	—	—	2.06 [2.027, 2.103]
Mixture with mucin 8% (w/w)	3	0.008 [0.0078, 0.0083]	0.042 [0.0390, 0.0452]	0.134 [0.1165, 0.1516]	38.95 [38.671, 39.232]
NaCMC 7% (w/w)	0	—	—	—	2.45 [2.431, 2.477]
Mixture with mucin 6% (w/w)	2	0.011 [0.0106, 0.0113]	0.094 [0.0923, 0.0965]	—	28.27 [28.204, 28.341]
Mixture with mucin 8% (w/w)	2	0.012 [0.0112, 0.0119]	0.078 [0.0773, 0.0797]	—	47.94 [47.860, 48.026]
Mixture with mucin 10% (w/w)	2	0.009 [0.0092, 0.0096]	0.061 [0.0603, 0.0623]	—	101.88 [101.64, 102.167]
NaCMC 8% (w/w)	1	0.690 [0.6405, 0.7386]	—	—	15.65 [15.488, 15.824]
Mixture with mucin 8% (w/w)	2	0.026 [0.0257, 0.0266]	0.179 [0.1729, 0.1851]	—	164.27 [163.474, 165.071]

Note: In square brackets, confidence intervals are reported.

straight lines (zero-order models) whose slope is equal to $1/\eta_N$. This indicates the lack of any elastic component in the sample behavior. On the contrary, the response of NaCMC l.v. grade solution prepared at the highest concentration (8% w/w) is described by a first-order model. This is likely due to the occurrence of further intermolecular physical entanglements and/or secondary chemical bonds when the polymer concentration increases. Such linkages provide rigidity to the sample structure, which then is characterized by a retarded elastic component. We also observed a growth in viscosity: the entangled polymer chains provide a higher resistance to flow.

For all the three NaCMC l.v. concentrations, the addition of mucin causes an increase in the elastic properties of the samples. In fact the creep curves of the mixtures are explained by higher order models with respect to the solutions of the polymer alone. This indicates the appearance in the mixtures of new structural units, due to physical and/or chemical interactions between polymer and mucin chains. The increase in n can be interpreted as an index of the extent of such interactions, which are also responsible for the increase in the η_N values.

In presence of mucin, a more pronounced increase in the elastic properties of the sample is observed for the lowest

Table III. NaCMC Medium Viscosity (m.v.) Grade: Model Order (n), Newtonian Viscosity (η_N), and Retarded Elastic Compliance Values (J_i , $i = 1, 2, 3$)

Sample	Model order n	Retarded elastic compliance (Pa^{-1})			Newtonian viscosity ($\text{Pa}\cdot\text{s}$) η_N
		J_1	J_2	J_3	
NaCMC 3% (w/w)	0	—	—	—	2.41 [2.385, 2.425]
Mixture with mucin 8% (w/w)	2	0.011 [0.0105, 0.0110]	0.076 [0.0745, 0.0767]	—	35.80 [35.750, 35.841]
NaCMC 3.4% (w/w)	1	0.339 [0.2139, 0.4647]	—	—	3.77 [3.675, 3.869]
Mixture with mucin 6% (w/w)	2	0.017 [0.0162, 0.0170]	0.139 [0.1356, 0.1417]	—	30.29 [30.222, 30.355]
Mixture with mucin 8% (w/w)	2	0.010 [0.0103, 0.0106]	0.066 [0.0653, 0.0676]	—	51.68 [51.555, 51.811]
Mixture with mucin 10% (w/w)	2	0.009 [0.0092, 0.0095]	0.055 [0.0537, 0.0555]	—	77.73 [77.542, 77.922]
NaCMC 4.1% (w/w)	1	0.454 [0.4311, 0.4776]	—	—	16.96 [16.802, 17.113]
Mixture with mucin 8% (w/w)	2	0.022 [0.0212, 0.0220]	0.259 [0.2513, 0.2671]	—	199.95 [198.944, 200.966]

Note: In square brackets, confidence intervals are reported.

Table IV. NaCMC High Viscosity (h.v.) Grade: Model Order (n), Newtonian Viscosity (η_N), and Retarded Elastic Compliance Values (J_i , $i = 1, 2, 3$)

Sample	Model order n	Retarded elastic compliance (Pa^{-1})			Newtonian viscosity ($\text{Pa}\cdot\text{s}$) η_N
		J_1	J_2	J_3	
NaCMC 1.4% (w/w)	1	0.303 [0.2923, 0.3136]	—	—	5.94 [5.896, 5.985]
Mixture with mucin 8% (w/w)	2	0.021 [0.0203, 0.0210]	0.150 [0.1464, 0.1537]	—	60.53 [60.204, 60.857]
NaCMC 1.6% (w/w)	2	0.065 [0.0615, 0.0689]	0.294 [0.2624, 0.3264]	—	20.29 [20.061, 20.527]
Mixture with mucin 6% (w/w)	2	0.023 [0.0222, 0.0231]	0.185 [0.1813, 0.1888]	—	83.99 [83.572, 84.413]
Mixture with mucin 8% (w/w)	2	0.026 [0.0250, 0.0261]	0.195 [0.1926, 0.1974]	—	156.83 [156.145, 157.518]
Mixture with mucin 10% (w/w)	2	0.010 [0.0101, 0.0105]	0.066 [0.0650, 0.0674]	—	259.66 [258.172, 261.167]
NaCMC 1.8% (w/w)	2	0.108 [0.1047, 0.1121]	1.021 [0.9576, 1.0838]	—	121.87 [119.103, 124.764]
Mixture with mucin 8% (w/w)	2	0.023 [0.0216, 0.0235]	0.189 [0.1837, 0.1939]	—	847.18 [838.859, 855.663]

Note: In square brackets, confidence intervals are reported.

NaCMC concentration (6% w/w) (n changes from 0 to 3); it indicates that stronger polymer-mucin interactions occur with respect to the higher concentrations. Such concentrations are characterized by a more entangled structure, which is highlighted by higher values of the viscoelastic parameters. The entanglement between polymer chains could hinder a deep interpenetration between polymer and mucin molecules, and interactions between NaCMC chains rather than between polymer and mucin could be favoured.

Let us observe that n does not change when the amount of mucin in the mixture increases, that is no new structural units form within the sample. This could indicate that no further types of linkage are involved in the interaction. However, a decrease in the J_i values, and an increase in the η_N values are observed: this means that a strengthening of the inner structure of the sample occurs. As new different types of interaction between polymer and mucin do not establish, such a strengthening is likely due to a greater number of the same chemical and/or physical bonds.

Medium Viscosity Grade (Table III)

As highlighted for the l.v. grade, the increase in polymer concentration is accompanied by an increase in both elastic and viscous properties of the sample. Let us observe that a retarded elastic component is already present at the medium concentration of NaCMC m.v. grade (3.4% w/w). On the contrary, such a component is absent for the corresponding isoviscous solution of NaCMC l.v. grade (7% w/w) (Table II). The higher molecular weight of m.v. grade chains would be responsible for a more rigid polymer network, characterized by higher elasticity.

For all the NaCMC m.v. grade solutions an increase in n is observed in presence of mucin. A greater variation of n occurs for the mixture which contains the lowest polymer concentration (3% w/w): this indicates a stronger polymer-mucin interaction. The minor entanglement of the polymeric chains, that occurs

at the low concentration, should facilitate the interpenetration phenomenon.

As observed for the l.v. grade, the presence of higher amount of mucin does not imply a change in n but a variation in the J_i and η_N values, which decrease and increase, respectively. These results confirm the assumption made for the l.v. grade: higher mucin concentrations produce a strengthening of polymeric network, but not the establishment of new structural units.

High Viscosity Grade (Table IV)

The NaCMC h.v. grade solutions prepared at different concentrations show a viscoelastic behavior described by one or more retarded elastic components. The model order of each solution is greater than that observed for the corresponding isoviscous solution of lower grades. Longer polymer chains are able to form also long-term interactions responsible for higher rigidity of the polymeric network.

Contrary to what we observed for the other two grades, the addition of mucin produces an increase in n only for the lowest concentration solution (1.4% w/w). This indicates that, only for this concentration, the interaction with mucin is such as to produce substantial changes in the retarded elastic response. This is due to a minor chain entanglement. However, a decrease in the J_i values and an increase in the η_N values are observed for the mixtures. Moreover, as already highlighted for the other two grades, a higher mucin concentration in the mixture is not accompanied by an increase in n but only by a variation of the J_i and η_N values.

The comparison between the three grades at the same concentration level confirms that, as already found in previous works (17,19), the viscosity grade affects the polymer-mucin interaction properties. The increase in n , observed in presence of mucin, is greater for the low grade, followed by the medium and high grades. The minor interaction properties of the high grade can be explained by the entanglement of high molecular

weight polymer chains, which hinders a deep interpenetration between the two macromolecular species. However, a deeper insight into the influence of polymer molecular weight would need an investigation about polymer polydispersity.

Dynamic Viscoelastic Measurements

Figure 4 compares the values of the dynamic interaction parameters ($\Delta G'/G'_{pol}$ and $\Delta G''/G''_{pol}$) calculated for the mixtures of the three grades of NaCMC which contain different polymer concentrations and 8% (w/w) mucin. For all the three grades both dynamic interaction parameters decrease when polymer concentration increases. Since $\Delta G'/G'_{pol}$ and $\Delta G''/G''_{pol}$ are generally considered as a measure of the extent of polymer-mucin interaction, the observed decrease means that a weaker interaction occurs when NaCMC concentration increases. The comparison of the three grades at the same concentration level shows that the increase in molecular weight is accompanied by a decrease in dynamic parameters. These results are in agreement with the model-based interpretation given for the creep curves.

Figure 5 compares the $\Delta G'/G'_{pol}$ and $\Delta G''/G''_{pol}$ values calculated for the mixtures of the three grades of NaCMC prepared at the same polymer concentration level, and with different mucin concentrations. For all the three grades both dynamic parameters increase when mucin concentration increases. This indicates that a strengthening of the polymer network occurs

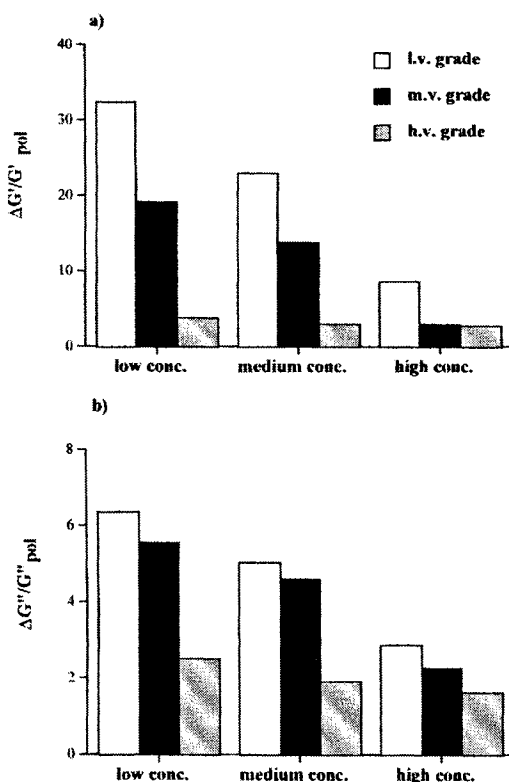


Fig. 4. Values of $\Delta G'/G'_{pol}$ (a) and $\Delta G''/G''_{pol}$ (b) calculated for the mixtures of the three viscosity grades of NaCMC which contain different polymer concentrations and 8% (w/w) mucin. Low concentration: 6.0% (w/w) l.v. grade, 3.0% (w/w) m.v. grade, 1.4% (w/w) h.v. grade. Medium concentration: 7.0% (w/w) l.v. grade, 3.4% (w/w) m.v. grade, 1.6% (w/w) h.v. grade. High concentration: 8.0% (w/w) l.v. grade, 4.1% (w/w) m.v. grade, 1.8% (w/w) h.v. grade.

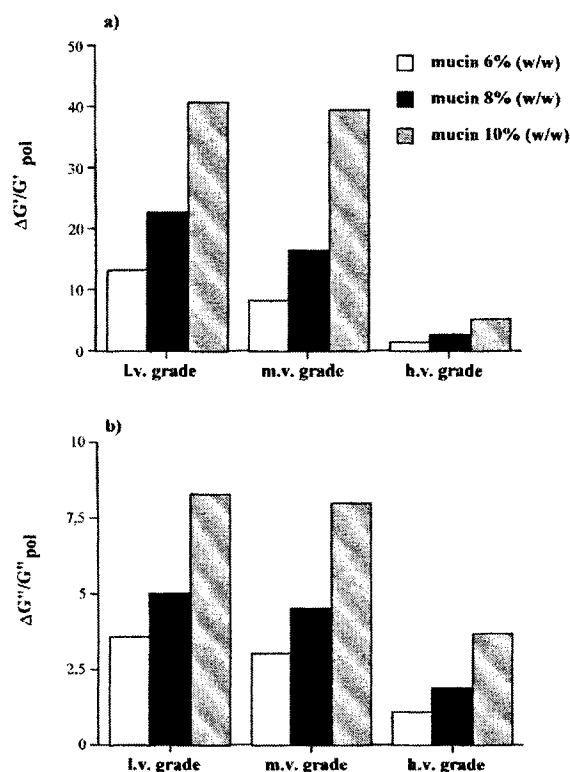


Fig. 5. Values of $\Delta G'/G'_{pol}$ (a) and $\Delta G''/G''_{pol}$ (b) calculated for the mixtures of the three viscosity grades of NaCMC which contain different mucin concentrations and the medium concentration of each polymer. Low grade: 7.0% (w/w). Medium grade: 3.4% (w/w). High grade: 1.6% (w/w).

as a result of the addition of increasing amounts of mucin. This is in line with the observed variation of the creep model parameters J_i and η_w (Tables II–IV).

Figure 5 confirms what illustrated in Fig. 4: the highest dynamic interaction is observed for the lowest grade.

Viscosity Measurements

Figures 6 and 7 show the values of rheological synergism calculated for the mixtures of the three grades, respectively prepared at different polymer concentrations with 8% (w/w) mucin, and at the same concentration level with different mucin concentrations.

In agreement with the results of our model-based study, $\Delta\eta/\eta_{pol}$ increases when either the polymer concentration or the molecular weight decrease, and also when mucin concentration increases.

CONCLUSIONS

Our model-based approach has allowed us to examine closely the interaction properties of sodium carboxymethylcellulose with porcine gastric mucin. Through the computational environment we have identified the most accurate models that describe the creep profiles of the various samples examined. It has enabled us to interpret the different viscoelastic responses of the samples. In particular, the model order and the values of the parameters have been considered: they indicate the number of structural units within the polymeric network and their strength, respectively. Therefore, they give a good description of

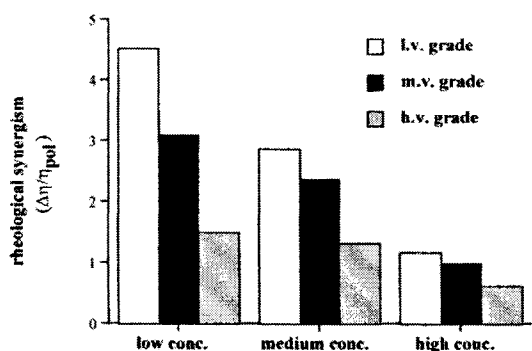


Fig. 6. Values of $\Delta\eta/\eta_{pol}$ calculated for the mixtures of the three viscosity grades of NaCMC which contain different polymer concentrations and 8% (w/w) mucin. Low concentration: 6.0% (w/w) l.v. grade, 3.0% (w/w) m.v. grade, 1.4% (w/w) h.v. grade. Medium concentration: 7.0% (w/w) l.v. grade, 3.4% (w/w) m.v. grade, 1.6% (w/w) h.v. grade. High concentration: 8.0% (w/w) l.v. grade, 4.1% (w/w) m.v. grade, 1.8% (w/w) h.v. grade.

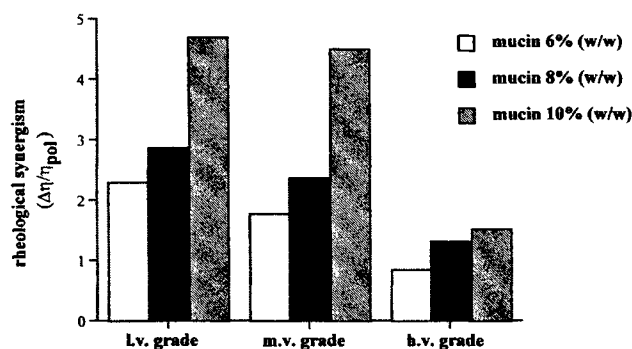


Fig. 7. Values of $\Delta\eta/\eta_{pol}$ calculated for the mixtures of the three viscosity grades of NaCMC which contain different mucin concentrations and the medium concentration of each polymer. Low grade: 7.0% (w/w). Medium grade: 3.4% (w/w). High grade: 1.6% (w/w).

the material complexity. The traditional rheological approach, based on viscosity and dynamic oscillatory measurements, had highlighted a strengthening of the mucoadhesive interface. In addition, our approach has allowed us to investigate more deeply the causes of such strengthening by providing further information about the structural variations that occur in the polymeric network. The strengthening of the mucoadhesive interface could be caused either by the establishment of new types of linkages accompanied by the formation within the sample of new structural units (evidenced by an increase in n) or by a greater rigidity of pre-existing linkages (indicated by a variation of the values of J_i and η_N not accompanied by a change in n).

Let us remark that the model-based approach has a general validity. It can be used to investigate a wide variety of phenomena involving structural variations revealed by changes in the material mechanical behavior.

REFERENCES

1. J. D. Smart, I. W. Kellaway, and H. E. C. Worthington. An in vitro investigation of mucosa-adhesive materials for use in controlled drug delivery. *J. Pharm. Pharmacol.* **36**:295–299 (1984).
2. H. Park and J. R. Robinson. Physico-chemical properties of water insoluble polymers important to mucin/epithelial adhesion. *J.*

Contr. Rel. **2**:47–57 (1985).

3. H. S. Ch'ng, H. Park, P. Kelly, and J. R. Robinson. Bioadhesive polymers as platforms for oral controlled drug delivery II: synthesis and evaluation of some swelling, water insoluble bioadhesive polymers. *J. Pharm. Sci.* **74**:399–405 (1985).
4. J. M. Gu, J. R. Robinson, and S. H. Leung. Binding of acrylic polymers to mucin/epithelial surfaces: structure-property relationships. *CRC Critical Reviews in Therapeutic Drug Carrier Systems* **5**:21–67 (1988).
5. D. Duchene, F. Touchard, and N. A. Peppas. Pharmaceutical and medical aspects of bioadhesive systems for drug administration. *Drug Dev. Ind. Pharm.* **14**:283–318 (1988).
6. C. Roberts, P. Buri, and N. A. Peppas. Experimental methods for bioadhesive testing of various polymers. *Acta Pharm. Technol.* **34**:95–98 (1988).
7. D. Duchene, G. Ponchel, D. Wouessidiewe, F. Lejoyeux, and N. A. Peppas. Méthodes d'évaluation de la bioadhésion et facteurs influents. *S.T.P. Pharma* **4**:688–697 (1988).
8. K. Dyvik and C. Graffner. Investigation of the applicability of a tensile testing machine for measuring mucoadhesive strength. *Acta Pharm. Nord* **4**:79–84 (1992).
9. Y. Jacques and P. Buri. Optimization of an ex vivo methods for bioadhesive quantification. *Eur. J. Pharm. Biopharm.* **38**:195–198 (1992).
10. N. A. Peppas and P. Buri. Surface, interfacial and molecular aspects of polymer bioadhesion on soft tissues. *J. Contr. Rel.* **2**:257–275 (1985).
11. C. M. Lehr, J. A. Bouwstra, H. E. Boddé, and H. E. Junginger. A surface energy analysis of mucoadhesion: Contact angle measurements on polycarbophil and pig intestinal mucosa in physiologically relevant fluids. *Pharm. Res.* **9**:70–75 (1992).
12. E. E. Hassan and J. M. Gallo. A simple rheological method for in vitro assessment of mucin-polymer bioadhesive bond strength. *Pharm. Res.* **7**:491–495 (1990).
13. S. A. Mortazavi, B. G. Carpenter, and J. D. Smart. An investigation of the rheological behaviour of the mucoadhesive-mucosal interface. *Int. J. Pharm.* **83**:221–225 (1992).
14. S. A. Mortazavi and J. D. Smart. Factors influencing gel strengthening at the mucoadhesive-mucus interface. *J. Pharm. Pharmacol.* **46**:86–90 (1994).
15. C. Caramella, M. C. Bonferoni, S. Rossi, and F. Ferrari. Rheological and tensile tests for the assessment of polymer-mucin interactions. *Eur. J. Biopharm. Pharm.* **40**:213–217 (1994).
16. F. Madsen, K. Eberth, and J. D. Smart. A rheological assessment of the nature of interactions between mucoadhesive polymers and a homogenized mucus gel. *Biomaterials* **19**:1083–1092 (1998).
17. S. Rossi, M. C. Bonferoni, F. Ferrari, M. Bertoni, and C. Caramella. Characterization of mucin interaction with three viscosity grades of sodium carboxymethylcellulose. Comparison between rheological and tensile testing. *Eur. J. Pharm. Sci.* **4**:189–196 (1996).
18. F. Ferrari, S. Rossi, A. Martini, L. Muggetti, R. D. Ponti, and C. Caramella. Technological induction of mucoadhesive properties on waxy starches by grinding. *Eur. J. Pharm. Sci.* **5**:277–285 (1997).
19. F. Ferrari, S. Rossi, M. C. Bonferoni, and C. Caramella. Characterization of rheological and mucoadhesive properties of three grades of chitosan hydrochloride. *Il Farmaco* **52**(6-7):493–497 (1997).
20. M. Reiner. Rheology. In S. Flügge (ed.), *Encyclopedia of Physics*. Springer, Berlin, 1958, volume 6, pp. 434–550.
21. A. Capelo, L. Ironi, and S. Tentoni. Automated mathematical modeling from experimental data: an application to material science. *IEEE Trans. SMC* **28**:356–370 (1998).
22. S. Rossi, M. C. Bonferoni, G. Lippoli, M. Bertoni, F. Ferrari, C. Caramella, U. Conte. Influence of mucin type on polymer-mucin rheological interactions. *Biomaterials* **16**:1073–1079 (1995).
23. L. Ironi and S. Tentoni. An integrated quantitative-qualitative approach to automated modeling of visco-elastic materials from experimental data. In R. Teti (ed.), *Proc. ICME 98 - CIRP International Seminar on Intelligent Computation in Manufacturing Engineering, Capri, 1–3 July 1998*. CUES-Salerno & RES Communication-Naples, 1998, pp. 381–388.
24. T. Söderström and P. Stoica. *System Identification*. Prentice-Hall, Cambridge, 1989.